

Emissions from the Fused Filament Fabrication 3D Printing with Lignocellulose/Polylactic Acid Filament

Qianqian Zhu,^{a,d} Qian Yao,^a Jun Liu,^a Jianzhong Sun,^{a,*} and Qianqian Wang^{a,b,c,*}

The application of Fused Filament Fabrication (FFF) 3D printing for offices, educational institutions, and small prototyping businesses has recently attracted increased attention. Thermal-fused filaments could emit potentially hazardous atmospheric particulate matter (PM) and volatile organic compounds (VOCs). This study evaluated the particle and VOCs emission characteristics of an FFF 3D printer with lignocellulose/polylactic acid (PLA) filament to reduce emissions. The PM2.5, PM0.2-10, and VOCs emission behaviors of the FFF 3D printer with a lignocellulose/PLA filament were investigated in a test chamber under different printing conditions. Pyrolysis-gas chromatography/mass spectrometry (Py-GC/MS) was applied to analyze the formation of VOCs from lignocellulose/PLA filaments. Analysis indicated that particle formation dominated the heating process, whereas VOCs were mainly released during the printing process. The results further showed that printing at higher relative humidity and high filament feeding temperatures triggered higher VOCs emissions. In addition, high humidity facilitated particle agglomeration and reduced PM concentration. Printing at higher filament feeding temperatures also resulted in high particle emissions. Finally, Py-GC/MS analysis determined the decomposition products of the lignocellulose/PLA filament corresponding to the main ingredients of VOCs.

Keywords: 3D printing; Lignocellulose filament; Particulate matter; Volatile organic compounds

Contact information: a: Biofuels Institute, School of the Environment and Safety Engineering, Jiangsu University, Zhenjiang 212013 China; b: State Key Laboratory of Pulp and Paper Engineering, South China University of Technology, Guangzhou 510640 China; c: Institute of Chemical Industry of Forest Products, Chinese Academy of Forestry, Jiangsu Key Laboratory of Biomass Energy and Material, Nanjing, 210042, China; d: Analysis and Testing Center, Jiangsu University, Zhenjiang, 212013 PR China; *Corresponding authors: Email: jzsun1002@ujs.edu.cn; qianqian.wz@gmail.com

INTRODUCTION

Three-dimensional (3D) printing, also known as additive manufacturing, enables easy, fast, and cost-effective fabrication of prototypes with complex shapes using computer-aided design (Wang *et al.* 2018). Therefore, 3D printing has become increasingly popular in educational institutions, small prototyping businesses, and quasi-industrial applications. Three-dimensional printing technologies can be categorized into binder jetting, directed energy deposition, material extrusion, material jetting, powder bed fusion, sheet lamination, and vat photopolymerization according to how the layers were deposited. Fused filament fabrication (FFF) is the most commonly used 3D-printing technology, and it mainly uses continuous polymer filaments such as polylactic acid (PLA) and acrylonitrile butadiene styrene (ABS) filaments as raw materials. The thermoplastic filament is first liquefied in a heating chamber and then deposited on a platform *via* an extrusion nozzle. Currently, desktop FFF 3D printers with thermoplastic filaments are frequently used because they are cheap and easy to operate. However, desktop 3D printers are often used

in poorly ventilated offices or homes. Much particulate matter (PM) and many volatile organic compounds (VOCs) are produced during the FFF 3D printing process (Azimi *et al.* 2016). In-depth studies on the potential health risks associated with FFF 3D printing exposure are needed.

Previous studies have focused on the emissions from FFF 3D printers with two commonly used PLA and ABS filaments under different conditions in test chambers (Deng *et al.* 2016; Byrley *et al.* 2019; Ding *et al.* 2019; Poikkimäki *et al.* 2019). Particle concentrations and size distributions were investigated with an aerosol dynamic model to understand particle formation and emission mechanisms (Zhang *et al.* 2018). Byrley *et al.* (2019) found that ABS filaments emitted higher concentrations of ultrafine particles than PLA filaments. Notably, no substantial difference in the mean size of ultrafine particles emitted from the filaments was detected. Steinle (2016) reported that printing with PLA filaments resulted in higher ultrafine aerosol emissions than printing with ABS filaments. Methylmethacrylate was the main ingredient among the total VOCs emitted when printing with PLA. For ABS, styrene was the predominant compound detected. The effects of infill on particle emissions were also systematically investigated. Lower infill height and higher infill density resulted in fewer particle emissions (Cheng *et al.* 2018). Kwon *et al.* (2017) suggested that FFF 3D printing at a low temperature with a low-emitting filament and ventilation control can reduce particle emissions.

Several kinds of lignocellulose-filled PLA filaments have been recently produced (Kariz *et al.* 2018; Wang *et al.* 2020). The addition of lignocellulose to FFF thermoplastic filament produced a wood-like appearance with enhanced physical properties; therefore, it is a more potentially cost-effective and less hazardous option than traditional plastic filaments. Different lignocellulose components, such as cellulose (Murphy and Collins 2018; Ambone *et al.* 2020), hemicellulose (Xu *et al.* 2018), and lignin (Li *et al.* 2016), were added to the PLA filaments, which resulted in excellent performance and broader potential applications. Cellulose nanomaterial, as a green nanofiller, can improve the properties of PLA filament and provide composite filaments with more functionalities (Wang *et al.* 2019a,b; Zhu *et al.* 2020a,b). PM2.5 emissions from lignocellulose biomass combustion have drawn much attention due to adverse health effects. PM2.5 pollutions, especially in winter, have caused serious socio-economic problems in China. The burning of lignocellulose produced large amounts of PM2.5 in an open environment (Chen *et al.* 2017). 3D printing with lignocellulose filament at a temperature that close to the degradation temperature of lignocellulose may produce large amount PM2.5 in poorly ventilated rooms. The impacts of 3D printing on indoor air quality are still unclear.

To properly evaluate the risk of exposure to PM and VOCs emissions from FFF 3D printers with lignocellulose filaments, it is essential to understand the factors that influence PM and VOCs emissions and their concentrations. The printing parameters and the properties of the thermoplastic filaments are the two most important factors that influence emissions. Wang *et al.* (2019a, 2020) reported that lignocellulose-filled PLA filaments were successfully fabricated. The thermal decomposition kinetics of lignocellulose/PLA filament were systematically examined, and their printability was evaluated. However, there have been few studies on the emissions of lignocellulose/PLA filaments in FFF 3D printing in the literature. Therefore, the primary aim of this study was to investigate the 3D printing parameters that influence emissions from desktop FFF 3D printers. Specifically, the printing-related parameters of filament feeding temperature, relative humidity, and printing failure were investigated to address the existing knowledge gaps.

EXPERIMENTAL

Materials

3D printer and lignocellulose/PLA filament

The FFF 3D printer used in this research was a commercial desktop 3D printer (M3036; Shenzhen Soongon Co., Ltd., Shenzhen, China) designed for small prototyping businesses, educational institutions, and quasi-industrial application. The printer had side doors but no cover on the top. The maximum size that it could print was 300 mm × 300 mm × 360 mm. The maximum temperatures for the print nozzle and hotbed were 250 °C and 120 °C, respectively. The lignocellulose/PLA filament tested in this study was an FS-B011 model lignocellulose/PLA filament obtained from Guangzhou Fly-Sheng Intelligent Technology Co., Ltd. (Guandong, China). The lignocellulose content was approximately 20 wt% of the filament. The density of the filament was 1.12 g/cm³. Other specific additives and mass fractions were not provided. According to the manufacturer, lignocellulose/PLA filament was used to print furniture related products due to its wood-like properties.

Test Chamber for 3D Printing Emission Measurement

All measurements were carried out in a homemade 3D printing test chamber. The ceiling door of the 3D printer was sealed with an anti-static acrylic panel. All the doors were tightly closed when printing. Additional tape was also applied to seal the possible leakage between the door and metal panel. An air inlet equipped with a HEPA-activated carbon membrane was installed. Humidity was controlled at 80 ± 3%, 70 ± 3%, 60 ± 3%, and 50 ± 3% by a humidifier (Model: GXZ-J260; Shenzhen Fenzeer Co., Ltd., Shenzhen, China). A small electric fan (mini battery fan, wind power, 2.5 m/s) was used to fully mix the air in the test chamber. Before each experiment, the chamber was carefully cleaned and flushed with fresh filtrated air for 30 mins. The volume of sealed space was approximately 0.18 m³.

3D Printing Parameters

A pre-printing feed operation of the filament was required to ensure that the molten filament could be smoothly extruded through the printing nozzle.

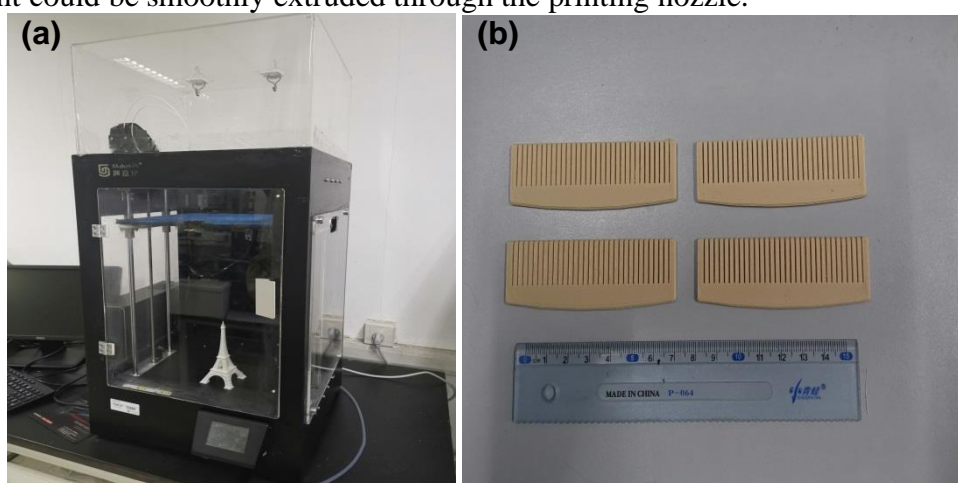


Fig. 1. The (a) MakerPi FFF 3D printer and (b) printed items

In each test, the 3D-printing process was divided into four stages, which included the pre-printing stage (30 min), the filament feeding stage (3 min), the printing stage (24 min), and the post-printing stage (33 min). The total time was 100 min. The filament feeding temperature, printing temperature, printing speed, and infill rate were 210 °C, 210 °C, 40 mm/s, and 100%, respectively, at 70% RM with a 0.4-mm nozzle unless otherwise specified. The print speed and bed temperature were 40 mm/s and 50 °C, respectively. The 3D printer and printed combs are shown in Fig. 1. Wooden combs are common in daily life. The 3D printed combs with lignocellulose/polylactic acid filaments exhibited wooden-like structures.

Emission Characterization

FFF 3D printing of lignocellulose/PLA filament at elevated temperatures may introduce a large amount micron-scale PM to indoor air quality, as compared with agriculture waste burning. The real-time mass concentrations of PM with a size of 2.5 microns (PM2.5) were determined *via* a DustTrak II aerosol monitor (Model: TSI 8530; TSI Inc., Shoreview, MN, USA). A Promo-3000 aerosol spectrometer (Palas GmbH, Karlsruhe, Germany) was used to measure the number concentration of PM ranging in size from 0.2 microns to 10 microns (PM0.2 to PM10) with the data recording intervals set to 1 s. The VOCs concentration was monitored using a MiniRAE 2000 photoionization detector with a data recording interval of 1 min. The PM released during printing was collected on a polycarbonate filter with a diameter of 47 mm and pore size of 0.1 mm (0.1 $\mu\text{m} \times 47 \text{ mm}$, GVS Filter Technology, Suzhou, China) at a flow rate of 2.5 L·min⁻¹. After sampling, the filter membrane was pasted on the scanning electron microscope (SEM) sample stage using conductive tape and spray-coated with gold (MSP-1S; Shinkku VD, Tokyo, Japan) for 10 min. The morphology of PM was observed *via* SEM-EDX (JSM-7800F; JEOL, Tokyo, Japan; EDAX, Mahwah, NJ, USA) at an acceleration voltage of 15 kV. In addition, pyrolysis-gas chromatography/mass spectrometry (Py-GC/MS) testing was adopted to pyrolyze the lignocellulose/PLA filament with a PY-2020iD pyrolyzer (Frontier Lab, Fukushima, Japan) and perform an analysis using a QP-2010 Ultra GC/MS (Shimadzu Corporation, Tokyo, Japan) with a DB-5ms column. To simulate the emissions of the lignocellulose filament during 3D printing, the pyrolysis temperature was set at 210 °C.

RESULTS AND DISCUSSION

Effect of Humidity on Emissions

Both PM and VOCs are emitted during FFF 3D printing, but the effect of relative humidity on such emission from lignocellulose/PLA filament has not been studied in detail. In this study, the effect of relative humidity on the emission from lignocellulose filament materials was evaluated (Fig. 2). The PM2.5 mass concentration increased rapidly during the filament feeding stage and reached the plateau within 1 min after the filament feeding stage. The PM2.5 mass concentration then steadily declined to their background levels. The highest PM2.5 mass concentration reached was 1500 $\mu\text{g}/\text{m}^3$ at 70% relative humidity. The relation between the peak PM2.5 emission and relative humidity was complicated.

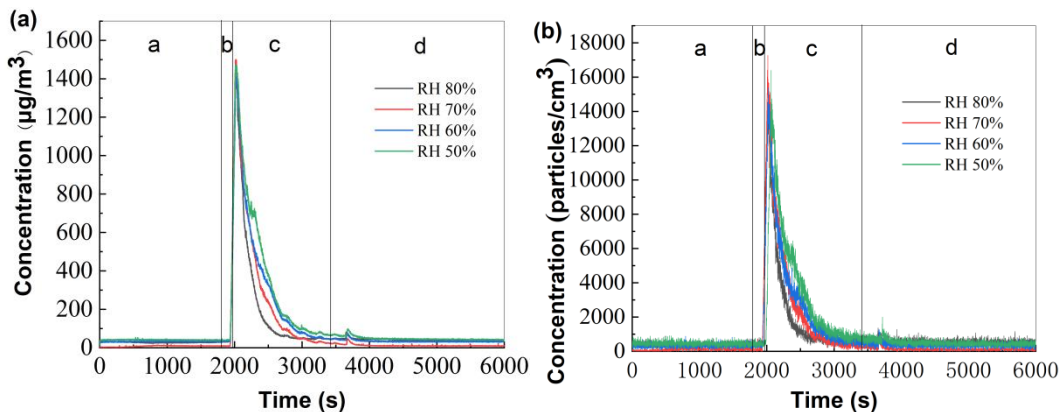


Fig. 2. The (a) PM2.5 mass concentration and (b) total particle number concentration of PM0.2 to PM10 at different humidity: a. Pre-printing stage; b. Filament feeding stage; c. Printing stage; d. Post-printing stage

Contrary to expectations, the PM2.5 mass concentrations steadily declined during the normal printing process, which may have indicated a lack of PM emissions. This may have been due to the rapid solidification of the melted filament on the platform during normal printing. A similar finding was reported by Stabile *et al.* (2017). It was reported that 3D printer emissions are dominated by particles with sizes in the nanoscale (Poikkimäki *et al.* 2019). Those nanoscaled particles acted as the building unit and quickly aggregated into large particles (*i.e.*, PM2.5) under different humidity (Rao *et al.* 2017). Relative humidity plays a crucial role in the aggregation of nanoscaled particles. The data indicated that high humidity could facilitate the aggregation of nanoscaled particles into large particles. The PM2.5 data under different humidity have implications in providing methods to control the particle emissions. Similar trends were also found in the total particle number concentration of PM0.2 to PM10 (Fig. 2b).

The SEM morphologies of the collected PM at different humidity are shown in Fig. 3. The PM had irregular shapes. The particle size collected at 80% relative humidity was larger than that collected at lower relative humidity, which indicated that humidity may have promoted the formation of large particles. Energy spectrum analysis showed that C and O were the main elemental components of the particles. Besides, there were small amounts of metallic elements, such as Fe, Ni, and Pt. The presence of these metallic elements may have been due to the additives in the filament. Alternatively, they may have been introduced during the spray coating process.

Figure 4 shows the concentration of VOCs emitted at different relative humidity. The data showed that VOCs concentration slightly increased in the filament feeding stage, which was followed by a rapid increase in the normal printing stage. This indicated that the lignocellulose/PLA filaments evaporated VOCs during both the feeding and printing process. The average temperature during the heating process was lower than the printing temperature. Filament extrusion or shearing helps to release the VOCs into the air. These two reasons contributed to the higher level of VOCs emission during printing, as compared with the heating stage. Further, the concentration of VOCs released during printing at higher relative humidity was higher than that of VOCs released at lower relative humidity conditions. The emitted particles may act as condensation nuclei under high humidity.

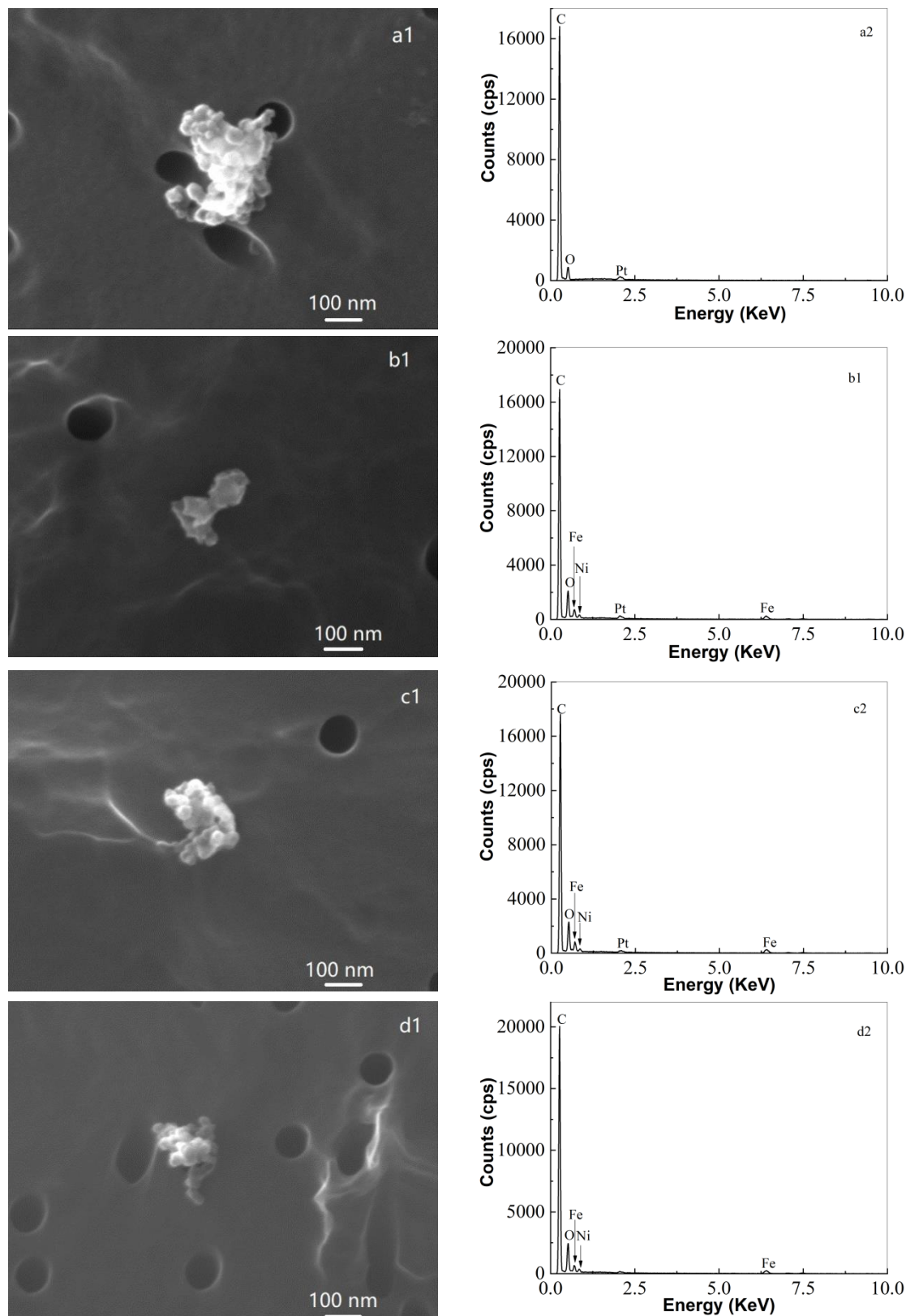


Fig. 3. The morphology (1) and elemental composition (2) of PM collected during 3D printing at different relative humidity (RH): (a) 80% RH; (b) 70% RH; (c) 60% RH; (d) 50% RH

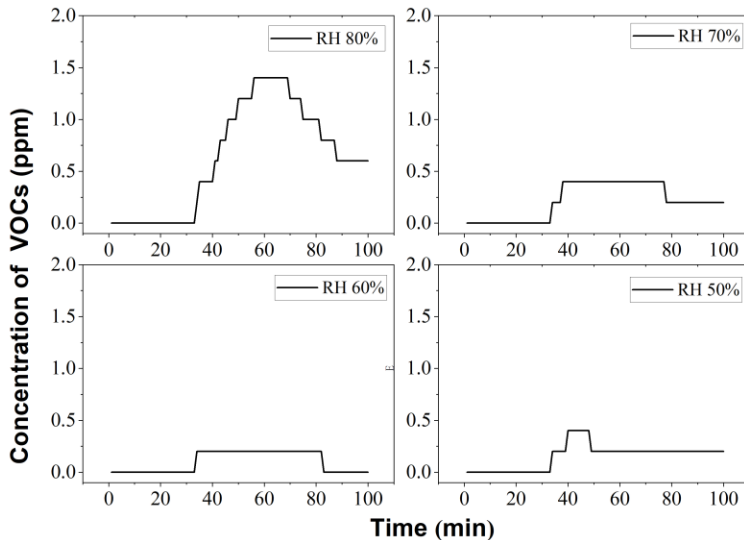


Fig. 4. The VOCs concentration during FFF 3D printing with lignocellulose/PLA filaments at different humidity

Effect of Filament Feeding Temperature on Emissions

The recommended printing temperature for lignocellulose/PLA filaments is 210 °C. When printing at temperatures lower than 210 °C, frequent nozzle clogging occurred, impeded the printing process seriously. The printing temperature was thus maintained at 210 °C. The impacts of printing temperature (nozzle temperature) on emissions have been extensively examined in previous studies (Jeon *et al.* 2020; Yi *et al.* 2019; Zhang *et al.* 2017). Thus, the impacts of filament feeding temperature on emissions were examined. Figure 5 shows that the peak value of PM2.5 and total particle number concentration (PM0.2 to PM10) emitted from the printing process with a filament feeding temperature of 180 °C were 119 µg/m³ and 1.6 × 10³ particles/cm³, respectively.

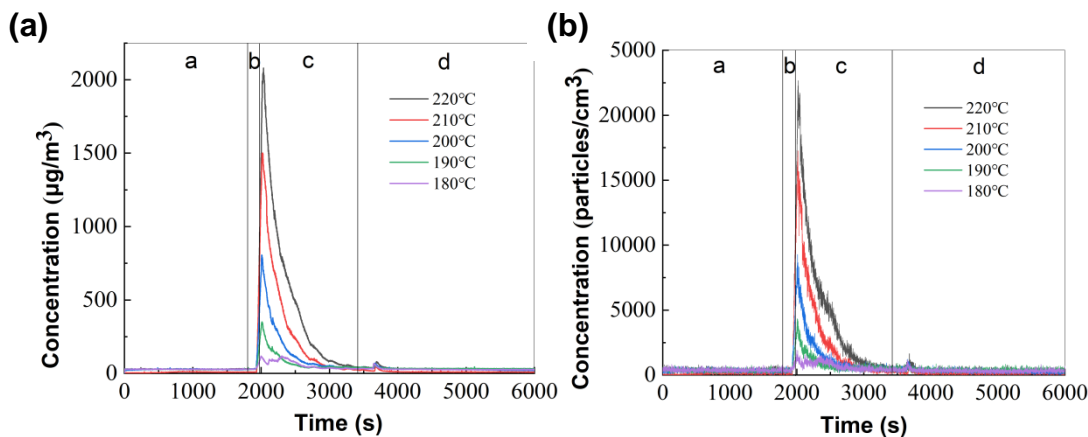


Fig. 5. The PM2.5 mass concentration and total particle number concentration of PM0.2 to PM10 at different filament feeding temperatures

As the filament feeding temperature increased, emissions of PM2.5 and PM0.2 to PM10 also increased rapidly. The PM2.5 and PM0.2 to PM10 emissions reached a plateau at 220 °C of 2080 µg/m³ and 2.3×10⁴ particles/cm³, which were 17.5 times and 14.4 times the emissions released at 180 °C, respectively. The particles released from

lignocellulose/PLA filaments increased as feeding temperature increased, which was closely related to the decomposition process of the filament. Al-Itty *et al.* (2012) reported that the decomposition temperature of PLA began at 200 °C and reached the maximum decomposition rate at 300 °C. The particle emissions were formed as products of the thermal decomposition, condensation, and subsequent particle growth to aggregates (Vance *et al.* 2017).

The effect of filament feeding temperature on VOCs emissions was examined. Figure 6 shows that VOCs emissions at higher temperatures were substantially higher than those at lower temperatures. To reduce the harmful PM and VOCs emissions from FFF 3D printing, it is recommended to start at the lowest filament feeding and printing temperature possible (Davis *et al.* 2019; Jeon *et al.* 2020).

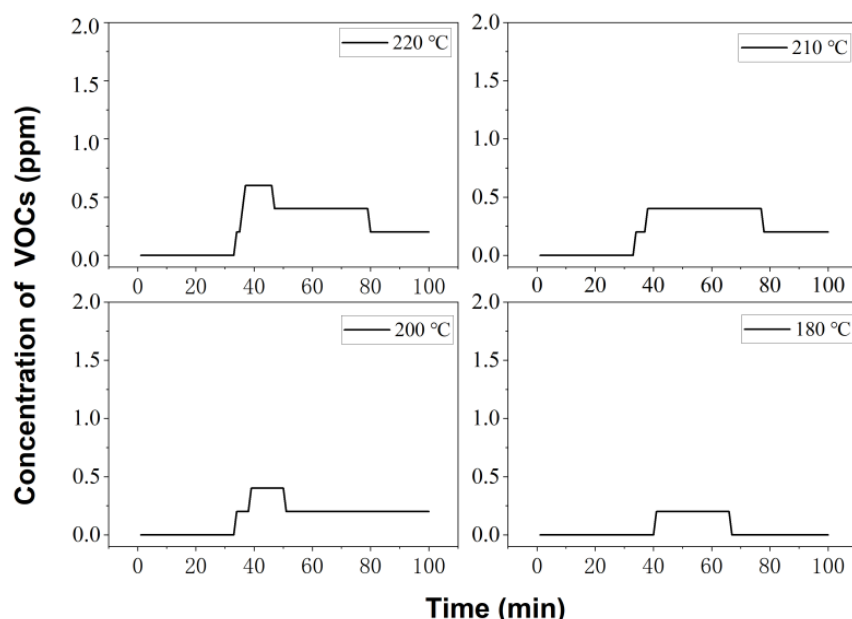


Fig. 6. The VOCs concentration during FFF 3D printing with lignocellulose/PLA filaments at different filament feeding temperatures

Effect of Printing Failure on Emissions

Figure 7 shows that printing failure can result in wasted filaments and broken prints. Nozzle clogging of the FFF 3D printer happened occasionally. Darker fibrous particles could be observed in the clogged nozzle after unloading. Nozzle clogging seriously affected print quality. In some extreme cases, terminating printing was the only effective way to solve the problem. Figure 8 shows the PM2.5 emissions from printing failure. When printing finished without unloading the filament, the PM2.5 mass concentration increased remarkably upon subsequent printing. The melted filament was not tightly bonded to the platform in the first layer of printing and may have adhered to the nozzle. Long time exposure to high temperatures of the melted filament resulted in higher PM2.5 emissions. Figure 8 shows that printing failure greatly increased the release of PM2.5. In conflict with the results of this study, Stefaniak *et al.* (2019) reported that printing failure resulted in fewer small particles and more large particles. Notably, the impacts of printing errors on emissions must be studied on a case-by-case basis because each case may be different.

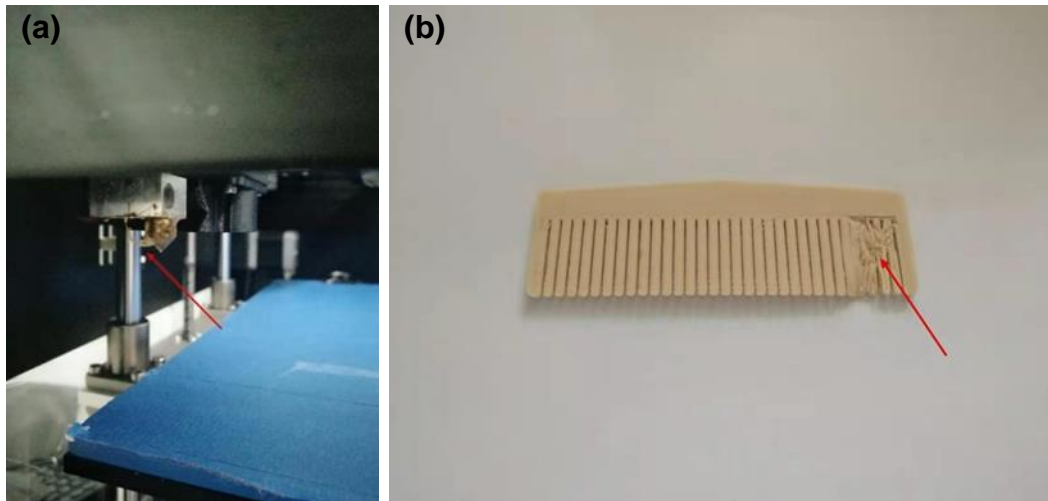


Fig. 7. The (a) clogged 3D printer nozzle and (b) broken prints

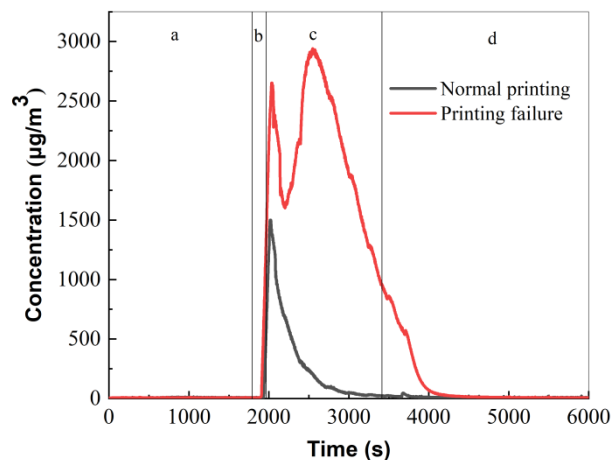


Fig. 8. The effect of printing failure on PM2.5 mass concentration

Analysis of VOCs Emissions by Py-GC/MS

To examine the formation of the main VOCs in the lignocellulose/PLA filament printing process, Py-GC/MS analysis was conducted on the filament. The ion chromatogram of pyrolyzed compounds from the lignocellulose filament at 210 °C is displayed in Fig. 9. Six main compounds were identified and characterized in Table 1. The main pyrolyzed compounds identified were L-lactide (4.85%), 1,6-dioxacyclododecane-7,12-dione (0.11%), dibutyl itaconate (0.06%), tributyl prop-1-ene-1,2,3-tricarboxylate (10.78%), tributyl citrate (1.07%), and acetyl tributyl citrate (83.02%). Both tributyl citrate and acetyl tributyl citrate are considered environmentally friendly non-toxic plasticizers. These are approved by the US Food and Drug Administration (FDA) and can be used in food packaging materials and medical appliances. Besides, L-lactide was also detected in the thermal decomposition of the lignocellulose/PLA filament. L-lactide is an important intermediate product for the synthesis of PLA. Inhalation of L-lactide can irritate the respiratory system. The health risks caused by these substances should be taken seriously when considering exposure to FMD 3D printing emissions.

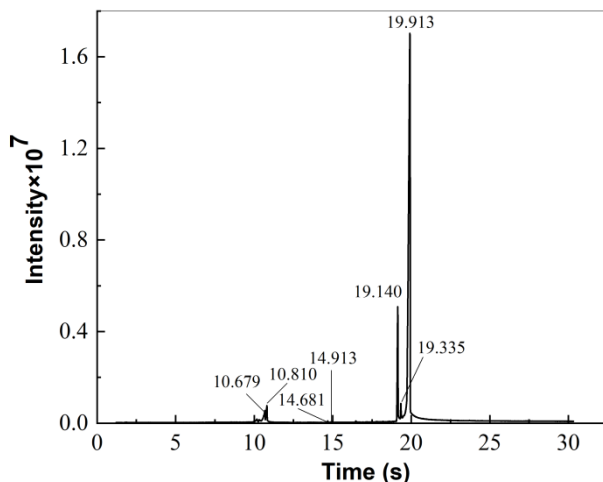


Fig. 9. Ion chromatogram of pyrolysis at 210 °C of lignocellulose/PLA filament

Table 1. Pyrolysis Products of Lignocellulose/PLA Filament at 210 °C

No.	Retention Time (min)	Chemical Abstracts Service (CAS) No.	Compound Name	Formula	Peak Area (%)
1	10.679	4511-42-6	L-Lactide	C ₆ H ₈ O ₄	2.40
2	10.810	4511-42-6	L-Lactide	C ₆ H ₈ O ₄	2.45
3	14.681	777-95-7	1,6-dioxacyclododecane-7,12-dione	C ₁₀ H ₁₆ O ₄	0.11
4	14.913	2155-60-4	Dibutyl itaconate	C ₁₃ H ₂₂ O ₄	0.06
5	19.140	7568-58-3	Tributyl prop-1-ene-1,2,3-tricarboxylate	C ₁₈ H ₃₀ O ₆	10.78
6	19.335	77-94-1	Tributyl citrate	C ₁₈ H ₃₂ O ₇	1.07
7	19.913	77-90-7	Acetyl tributyl citrate	C ₂₀ H ₃₄ O ₈	83.02

CONCLUSIONS

1. Large amounts of particulate matter (PM) and volatile organic compounds (VOCs) were emitted from FFF 3D printing with lignocellulose/poly(lactic acid) (PLA) filaments. Therefore, indoor air quality must be closely monitored during this process. It is strongly recommended to use the 3D printer only in a well-ventilated environment.
2. Particulate matter emissions were mainly released in the pre-printing stage rather than the printing stage, whereas VOCs were mainly released in the printing stage. High humidity facilitated the rapid decrease in PM level. The particulate matter particles captured under high humidity were larger than those captured under low humidity.
3. High filament feeding temperature and printing failure substantially increased the PM and VOCs emissions. Therefore, it is recommended to use low temperatures if possible.
4. The major VOCs compounds emitted from the lignocellulose/PLA filament were acetyltributylcitrate, tributyl prop-1-ene-1,2,3-tricarboxylate, and L-lactide.

ACKNOWLEDGMENTS

This work was supported by the National Key R&D Program of China (2018YFE0107100), the State Key Laboratory of Pulp and Paper Engineering (202003), the South China University of Technology, the Key Laboratory of Biomass Energy and Material of Jiangsu Province (JSBEM202012), and the Institute of Chemical Industry of Forest Products.

REFERENCES CITED

- Al-Ittry, R., Lamnawar, K., and Maazouz, A. (2012). "Improvement of thermal stability, rheological and mechanical properties of PLA, PBAT and their blends by reactive extrusion with functionalized epoxy," *Polymer Degradation and Stability* 97(10), 1898-1914. DOI: 10.1016/j.polymdegradstab.2012.06.028
- Ambone, T., Torris, A., and Shanmuganathan, K. (2020). "Enhancing the mechanical properties of 3D printed polylactic acid using nanocellulose," *Polymer Engineering and Science*, Early view (Online). DOI: 10.1002/pen.25421
- Azimi, P., Zhao, D., Pouzet, C., Crain, N. E., and Stephens, B. (2016). "Emissions of ultrafine particles and volatile organic compounds from commercially available desktop three-dimensional printers with multiple filaments," *Environmental Science & Technology* 50(3), 1260-1268. DOI: 10.1021/acs.est.5b04983
- Byrley, P., George, B. J., Boyes, W. K., and Rogers, K. (2019). "Particle emissions from fused deposition modeling 3D printers: Evaluation and meta-analysis," *Science of The Total Environment* 655, 395-407. DOI: 10.1016/j.scitotenv.2018.11.070
- Chen, J., Li, C., Ristovski, Z., Milic, A., Gu, Y., Islam, M. S., Wang, S., Hao, J., Zhang, H., He, C., Guo, H., Fu, H., Miljevic, B., Morawska, L., Thai, P., Lam, Y. F., Pereira, G., Ding, A., Huang, X., and Dumka, U. C. (2017). "A review of biomass burning: Emissions and impacts on air quality, health and climate in china," *Science of the Total Environment* 579, 1000-1034. DOI: 10.1016/j.scitotenv.2016.11.025
- Cheng, Y.-L., Zhang, L.-C., Chen, F., and Tseng, Y.-H. (2018). "Particle emissions of material-extrusion-type desktop 3d printing: The effects of infill," *International Journal of Precision Engineering and Manufacturing-Green Technology* 5(4), 487-497. DOI: 10.1007/s40684-018-0052-3
- Davis, A. Y., Zhang, Q., Wong, J. P. S., Weber, R. J., and Black, M. S. (2019). "Characterization of volatile organic compound emissions from consumer level material extrusion 3D printers," *Building and Environment* 160, Article ID 106209. DOI: 10.1016/j.buildenv.2019.106209
- Deng, Y., Cao, S.-J., Chen, A., and Guo, Y. (2016). "The impact of manufacturing parameters on submicron particle emissions from a desktop 3D printer in the perspective of emission reduction," *Building and Environment* 104, 311-319. DOI: 10.1016/j.buildenv.2016.05.021
- Ding, S., Ng, B. F., Shang, X., Liu, H., Lu, X., and Wan, M. P. (2019). "The characteristics and formation mechanisms of emissions from thermal decomposition of 3D printer polymer filaments," *Science of The Total Environment* 692, 984-994. DOI: 10.1016/j.scitotenv.2019.07.257

- Jeon, H., Park, J., Kim, S., Park, K., and Yoon, C. (2020). "Effect of nozzle temperature on the emission rate of ultrafine particles during 3D printing," *Indoor Air* 30(2), 306-314. DOI: 10.1111/ina.12624
- Kariz, M., Sernek, M., Obućina, M., and Kuzman, M. K. (2018). "Effect of wood content in FDM filament on properties of 3D printed parts," *Materials Today Communications* 14, 135-140. DOI: 10.1016/j.mtcomm.2017.12.016
- Kwon, O., Yoon, C., Ham, S., Park, J., Lee, J., Yoo, D., and Kim, Y. (2017). "Characterization and control of nanoparticle emission during 3D printing," *Environmental Science & Technology* 51(18), 10357-10368. DOI: 10.1021/acs.est.7b01454
- Li, T., Aspler, J., Kingsland, A., Cormier, L. M., and Zou, X. (2016). "3D printing - A review of technologies, markets, and opportunities for the forest industry," *Journal of Science & Technology for Forest Products and Processes* 5(2), 30-37.
- Murphy, C. A., and Collins, M. N. (2018). "Microcrystalline cellulose reinforced polylactic acid biocomposite filaments for 3D printing," *Polymer Composites* 39(4), 1311-1320. DOI: 10.1002/pc.24069
- Poikkimäki, M., Koljonen, V., Leskinen, N., Närhi, M., Kangasniemi, O., Kausiala, O., and Dal Maso, M. (2019). "Nanocluster aerosol emissions of a 3D printer," *Environmental Science & Technology* 53(23), 13618-13628. DOI: 10.1021/acs.est.9b05317
- Rao, C., Gu, F., Zhao, P., Sharmin, N., Gu, H., and Fu, J. (2017). "Capturing pm2.5 emissions from 3d printing via nanofiber-based air filter," *Scientific Reports* 7(1), 10366. DOI: 10.1038/s41598-017-10995-7
- Stabile, L., Scungio, M., Buonanno, G., Arpino, F., and Ficco, G. (2017). "Airborne particle emission of a commercial 3D printer: The effect of filament material and printing temperature," *Indoor Air* 27(2), 398-408. DOI: 10.1111/ina.12310
- Stefaniak, A. B., Johnson, A. R., Du Preez, S., Hammond, D. R., Wells, J. R., Ham, J. E., LeBouf, R. F., Menchaca, K. W., Martin, Jr., S. B., and Duling, M. G., et al. (2019). "Evaluation of emissions and exposures at workplaces using desktop 3-dimensional printers," *Journal of Chemical Health and Safety* 26(2), 19-30. DOI: 10.1016/j.jchas.2018.11.001
- Steinle, P. (2016). "Characterization of emissions from a desktop 3D printer and indoor air measurements in office settings," *Journal of Occupational and Environmental Hygiene* 13(2), 121-132. DOI: 10.1080/15459624.2015.1091957
- Vance, M. E., Pegues, V., Van Montfrans, S., Leng, W., and Marr, L. C. (2017). "Aerosol emissions from fuse-deposition modeling 3D printers in a chamber and in real indoor environments," *Environmental Science & Technology* 51(17), 9516-9523. DOI: 10.1021/acs.est.7b01546
- Wang, Q., Sun, J., Yao, Q., Ji, C., Liu, J., and Zhu, Q. (2018). "3D printing with cellulose materials," *Cellulose* 25(8), 4275-4301. DOI: 10.1007/s10570-018-1888-y
- Wang, Q., Ji, C., Sun, J., Yao, Q., Liu, J., Saeed, R. M. Y., and Zhu, Q. (2019a). "Kinetic thermal behavior of nanocellulose filled polylactic acid filament for fused filament fabrication 3D printing," *Journal of Applied Polymer Science* 137(7), Article ID 48374. DOI: 10.1002/app.48374
- Wang, Q., Yao, Q., Liu, J., Sun, J., Zhu, Q., and Chen, H. (2019b). "Processing nanocellulose to bulk materials: A review," *Cellulose* 26(13-14), 7585-7617. DOI: 10.1007/s10570-019-02642-3

- Wang, Q., Ji, C., Sun, L., Sun, J., and Liu, J. (2020). "Cellulose nanofibrils filled poly(lactic acid) biocomposite filament for FDM 3D printing," *Molecules* 25(10), Article number 2319. DOI: 10.3390/molecules25102319
- Xu, W., Pranovich, A., Uppstu, P., Wang, X., Kronlund, D., Hemming, J., Öblom, H., Moritz, N., Preis, M., and Sandler, N., *et al.* (2018). "Novel biorenewable composite of wood polysaccharide and polylactic acid for three dimensional printing," *Carbohydrate Polymers* 187, 51-58. DOI: 10.1016/j.carbpol.2018.01.069
- Yi, J., Duling, M. G., Bowers, L. N., Knepp, A. K., LeBouf, R. F., Nurkiewicz, T. R., Ranpara, A., Luxton, T., Martin, S. B., Jr., Burns, D. A., Peloquin, D. M., Baumann, E. J., Virji, M. A. and Stefaniak, A. B. (2019). "Particle and organic vapor emissions from children's 3-d pen and 3-d printer toys," *Inhalation Toxicology* 31(13-14), 432-445. DOI: 10.1080/08958378.2019.1705441
- Zhang, Q., Sharma, G., Wong, J. P. S., Davis, A. Y., Black, M. S., Biswas, P., and Weber, R. J. (2018). "Investigating particle emissions and aerosol dynamics from a consumer fused deposition modeling 3D printer with a lognormal moment aerosol model," *Aerosol Science and Technology* 52(10), 1099-1111. DOI: 10.1080/02786826.2018.1464115
- Zhang, Q., Wong, J. P. S., Davis, A. Y., Black, M. S. and Weber, R. J. (2017). "Characterization of particle emissions from consumer fused deposition modeling 3d printers," *Aerosol Science and Technology* 51(11), 1275-1286. DOI: 10.1080/02786826.2017.1342029
- Zhu, Q., Liu, S., Sun, J., Liu, J., Kirubaharan, C. J., Chen, H., Xu, W., and Wang, Q. (2020a). "Stimuli-responsive cellulose nanomaterials for smart applications," *Carbohydrate Polymers* 235, Article ID 115933. DOI: 10.1016/j.carbpol.2020.115933
- Zhu, Q., Yao, Q., Sun, J., Chen, H., Xu, W., Liu, J., and Wang, Q. (2020b). "Stimuli induced cellulose nanomaterials alignment and its emerging applications: A review," *Carbohydrate Polymers* 230, Article ID 115609. DOI: 10.1016/j.carbpol.2019.115609

Article submitted: June 23, 2020; Peer review completed: August 3, 2020; Revised version received: August 8, 2020; Accepted: August 9, 2020; Published: August 13, 2020.

DOI: 10.15376/biores.15.4.7560-7572